AN INVESTIGATION OF THE CRYSTAL STRUCTURE OF $Mn_2P_2O_7$

AN INVESTIGATION OF THE CRYSTAL STRUCTURE OF $Mn_2P_2O_7$

by

VINOD KUMAR TONDON, B.Sc.

A Thesis

Submitted to the Faculty of Graduate Studies

in Partial Fulfilment of the Requirements

for the Degree

Master of Science

McMaster University

May 1971

MASTER OF SCIENCE (1971) McMASTER UNIVERSITY
(Physics) Hamilton, Ontario

TITLE: An investigation of the crystal structure of $Mn_2P_2O_7$

AUTHOR: Vinod Kumar Tondon, B.Sc. (Agra University)

SUPERVISOR: Professor C. Calvo

NUMBER OF PAGES: vi, 59

SCOPE AND CONTENTS:

$Mn_2P_2O_7$ belongs to the monoclinic space group C2/m. The manganese atoms are six-fold coordinated to oxygen atoms forming distorted octahedra. The bonding in $P_2O_7^{4-}$ ion is discussed with refernece to values predicted by Cruickshank and Baur.

The central oxygen atom in $P_2O_7^{4-}$ ion shows enhanced motion, a feature common to all the members of the thortveitite series. By collecting X-ray data at -180°C, an attempt has been made to understand the nature of this enhanced motion.

ACKNOWLEDGEMENTS

I would like to express my sincere gratitude to Professor C. Calvo for his helpful guidance throughout the course of this work. Furthermore, I am indebted to him for his encouragement during many depressing moments.

My thanks are due to Dr. A. Prakash, for his help in handling the low temperature apparatus and in many other ways.

I would like to acknowledge the receipt of a graduate fellowship of the McMaster University.

I thank Mrs. H. Kennelly for typing this thesis.

TABLE OF CONTENTS

LIST OF TABLES

LIST OF ILLUSTRATIONS

CHAPTER 1

INTRODUCTION

Crystals of composition $X_2Y_2O_7$, where Y is generally the more electronegative cation, fall into one of the three classes, depending upon ionic radii of the Y and X atoms. Crystals for which the ionic radius of Y atom is greater than 0.60 Å crystallise into such structures as pyrochlore (Wyckoff, 1960) and weberite (Wyckoff, 1960), in which the Y atom is octahedrally coordinated. Crystals for which the Y atom is smaller than 0.60 Å, and X has an ionic radius greater than 0.97 Å, usually crystallize in one of a series of related structures, called dichromate structures (Brown and Calvo, 1970), and if X has an ionic radius smaller than 0.97 Å, they tend to crystallize in one of the structures related to that of the mineral thortveitite the class to which $Mn_2P_2O_7$, the subject of study in this thesis, belongs. In both of these structures, the Y ion lies in a tetrahedrally coordinated site, with tetrahedra sharing one oxygen atom per pair. The two families differ in that in the dichromate series the two tetrahedran tend to be in an eclipsed configuration, while they are nearly, and in some cases, exactly staggered for the thortveitite series.

The investigation of crystal structure of $Mn_2P_2O_7$

at room and low temperature is part of the programme in this group aimed at understanding the crystal chemistry and phase transformations of pyrocompounds. These pyrocompounds show a broad range of behaviour, but still have sufficient crystallographic similarity, which makes it possible to draw conclusions regarding the nature of extent of various factors, influencing the structure of this class.

The pyrophosphate, diarsenate and divanadate compounds included in this category are easily prepared in the laboratory, although naturally occuring ones only include thortveitite $(Sc,Y)_2Si_2O_7$ (Zachariasen, 1930; Cruickshank et al, 1962) and cherveitite $Pb_2V_2O_7$ mineral (Kawahara, 1967) which is a dichromate structure.

The structures in this category that have been studied so far, include diarsenates of Zn (Calvo, private communication) and Mg (Calvo and Neelkantan, 1967), the divanadates of Zn (Gopal, 1970), Cd (Au and Calvo, 1967) and Mn (Ebba Dorm et al, 1967), and the pyrophosphates of Cu (Lukaszewicz, 1966), Mg (Calvo, 1965a), Zn (Calvo, 1965b), Ni (Pietrazko et al, 1968) and Co (Krishnamachari and Calvo, 1970). $Mn_2P_2O_7$ has also been studied by Lukaszewicz and Smajkiewicz, although the atomic coordinates have not been well refined, in part because the data are incomplete.

The high temperature form of these pyrocompounds is the so called β form (thortveitite) and these are isostructural.

The low temperature phases are the so called α form and have four unique, although closely related structures. The α form has, unlike the β phase, a bent central P-O-P bond. Further in the α phase, the c axis roughly doubles with a c-glide plane replacing the mirror plane of β phase. $Mn_2P_2O_7$ is unique, among the pyrophosphates, in the sense that it apparently exists in one form, the β form, down at least 100°K, and does not show the usual α and β phases existing among others.

A difficulty, which is common to any of the compounds of the β form, is the space group ambiguity. It is easy to limit the space group to one of three choices Cm, C2 or C2/m taking into account symmetry of the diffracted rays, along with extinctions. It is only in C2/m space group that the anion $(P_2O_7)^{4-}$ must be linear, or at least appear to be on the average, with the central oxygen atom at the centre of symmetry.

Zachariasen chose C2/m, the only centrosymmetric space group possibility of the three, as the space group for thortveitite. This was later supported by work of Cruickshank, Lynton and Barclay (1962). The agreement between the observed and calculated structure factors for structures refined in each of these space groups was nearly the same. However, since the discrepancy between chemically equivalent bonds in the anions was unreasonable in the structure refined in space group Cm, and O-Si-O angles between chemically equivalent oxygen

atoms at the two ends of anions differed by a considerable amount in the case of C2 space group, it was concluded that the C2/m space group is the most favourable one, from stereochemical point of view. Later, Hamilton in 1965, discussed thortveitite as an example of the application of his significance tests and concluded that the space groups Cm or C2 do not provide a better model at 25% significance level. Hence C2/m is probably the correct space group. The slightly lower R values in Cm and C2 are because of the extra number of parameters used in refining these models. In the case of $\beta Zn_2P_2O_7$ (Chambers, Datars and Calvo, 1964) and β-$Mg_2P_2O_7$ (Calvo, Leung and Datars, 1967) and for thortveitite (Datars and Calvo, 1967) the choice of C2/m as the space group has been confirmed by electron paramagnetic resonance (e.p.r.) studies. $Zn_2P_2O_7$ and $Mg_2P_2O_7$ were doped with Mn^{+2}, while thortveitite itself has Fe^{+3} and Mn^{+2} impurities. In these β phases only one site is seen for the paramagnetic ion and this is consistent only with higher symmetry of space group C2/m. Since $Mn_2P_2O_7$ is paramagnetic and therefore e.p.r. studies are precluded, anomalous dispersion study of $Mn_2P_2O_7$ using CoKα radiation was carried out (Calvo, 1967) and space group was confirmed to be C2/m.

In view of the importance of the structure of thortveitite, for pyrocompounds with tetrahedrally disposed Y

atoms, we briefly review this structure. Chemically thortveitite is $(Sc,Y)_2Si_2O_7$, with appreciable replacement of Sc^{+3} and Y^{+3} by Fe^{+3} and Mn^{+2}. The crystal is monoclinic with systematic absences of reflections of the type $hk\ell$ when h+k = odd and has C2/m space group. In this space group, the central oxygen atom of the anion, $Si_2O_7^{-6}$, lies on centre of symmetry and hence the Si-O-Si bond must be linear (Angle Si-O-Si = 180°). The anion is thus forced to have a staggered configuration. The cations have an irregular octahedral environment. These irregular octahedra share edges to form a pseudo-hexagonal network extending in the (001) plane. Only two thirds of the hexagonal holes, formed by a double layer of close packed oxygen atoms are occupied by cations. Adjacent sheets of these octahedra are joined by sharing oxygen atoms with the pyrosilicate ions.

The structure may be described, alternatively, by a set of layers of separation $\underline{a}/2$ ($\sim$3.3 Å) and which contain the unit cell vectors $\underline{b}$ and $\underline{c}$ (See Figure 1-1). These layers contain pairs of cation octahedra which share one edge. The two remaining shared edges join adjacent layers. These cation pairs are linked together in the layer by $Si_2O_7^{-6}$ anions. The shared oxygen atom of the pyro ion has been labelled the "01" atom. One of the terminal oxygen atoms at each end of the ion lies in a mirror plane as do the Si atoms. These oxygen atoms are labelled the "02" atoms and are the oxygen atoms

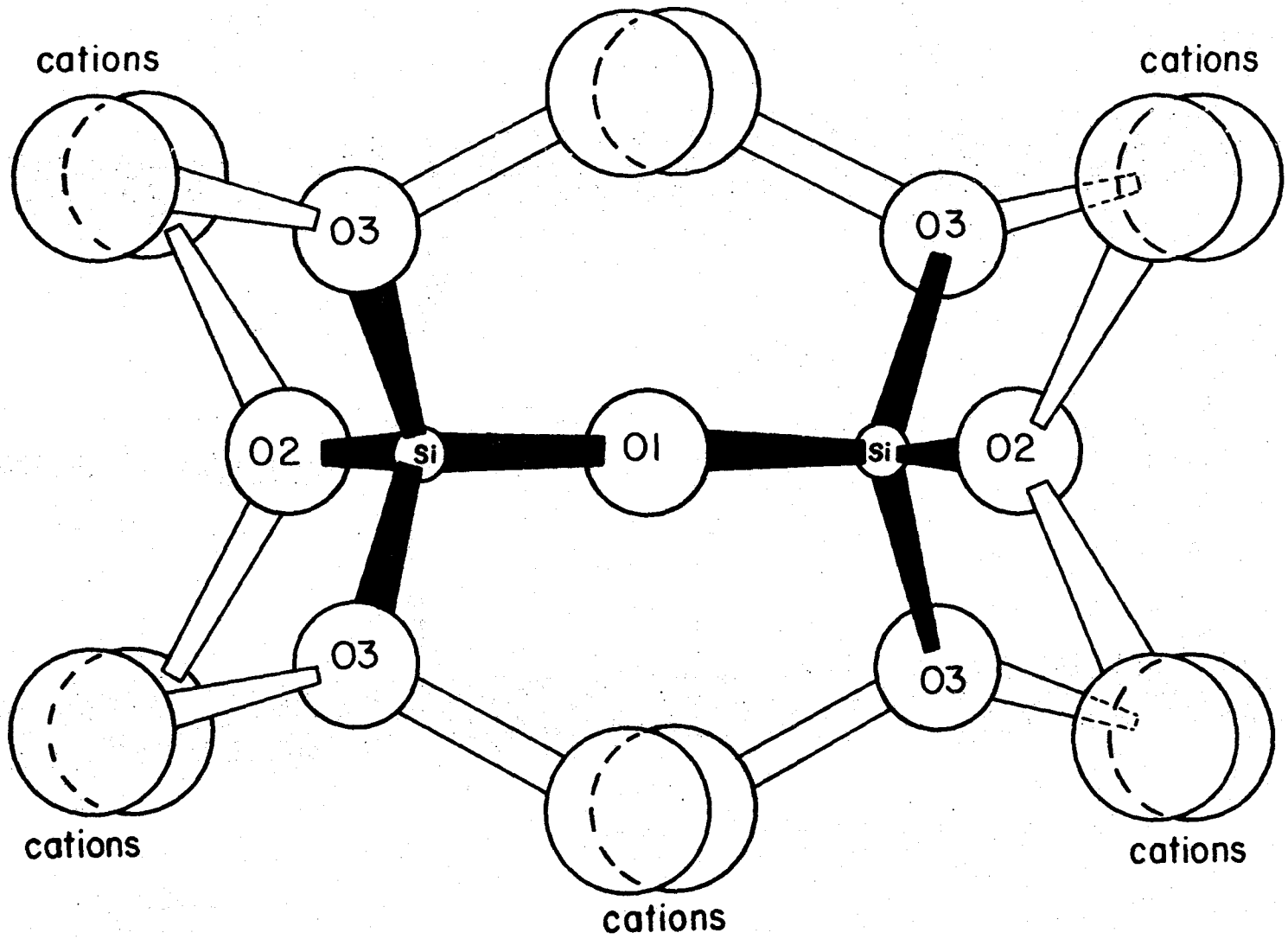

FIGURE I-1

The structure of the thortveitite mineral

involved in the shared edge. The remaining four oxygen atoms which are related in pairs by mirror plane are labelled the "03" atoms. The cation pairs are connected along the b direction by '03' atom at one end of the anion. This pattern is repeated since the central oxygen atom '01' lies at a centre of symmetry. These layers are joined to one another by additional cation-oxygen bonds. This description is applicable to all the high temperature forms of the 'small cation' pyrophosphates (β form).

Cruickshank (1961) has discussed the nature of bonding in compounds of thortveitite type, where Y is Si, S, Cl or P atom, in an anion $Y_2O_7^{-n}$. In an isolated tetrahedron four σ bonds to oxygen atoms, for example, are formed with sp^3 hybridisation of orbitals of the Y atom. The d_γ orbitals of the central atom and 2pπ orbitals of oxygen are used to form two π bonds. A lone pair is still left on each oxygen atom, which may be used to bond with the cation atoms in a solid phase. The pyro group is formed by joining two PO_4^{-3} tetrahedra so as to share one oxygen atom (central oxygen atom 01). In this shared anion, the degree of π bonding varies with state of hybridisation of central oxygen atom. If the angle subtended by two Y atoms at the central oxygen atom is tetrahedral angle (≃ 109°25'), 01 atom would be sp^3 hybridized and unable to support π bonding with 3d orbitals

of Y atom. If the angle subtended is 120°, 01 atom would be sp^2 hybridized, and one of two π bonds in each tetrahedra is joined across the atom. When angle is 180°, 01 atom is sp hybridized and both π bonds are joined across the atom. As the amount of π bonding to the shared oxygen atom increases, its bond distances to Y atoms are decreased and bond length to the terminal oxygen atoms are increased.

Cruickshank has predicted bond lengths for the P-O(-P) and terminal P-O bonds for each of these hybridization schemes, based on valence bond theory. He obtains 1.64 Å and 1.51 Å for P-O(-P) and P-O bond lengths respectively when the P-O-P angle is 120° and 1.58 Å and 1.53 Å when the P-O-P angle is 180°, without taking into account the effect of the environment The actual configuration adopted by an anion when put in a crystal field would be a balance of reasonable close packing of anions with cations and stability of anion in different configurations to form a translationally invariant three dimensional crystal.

Recently Baur (1970) suggested that for a given coordination number of X around A, the values of individual distances d(A-X) vary directly with the p_X values which are being received by the individual anion X, where p_X is defined as

$$p_X = \sum_i s_X^i = \sum_i \frac{z_c^i}{(C.N.)_c^i} .$$

The summation is over all the near neighbour cations surrounding the anion X, Z_c^i is the formal charge, and $(C.N.)_c^i$ is the coordination number of ith cation C. The bond lengths d(A-X) can be predicted to an average accuracy of about 0.02 Å, using equation of the form

$$d(A-X) = (a+bp_X)$$

a and b being empirical constants for a particular pair of A and X.

Since for P-O pair a = 1.32, b = 0.11 one has $d(P-O) = 1.32 + 0.11\ p_X$ and for a typical β phase $p_{01} = 2.5$, $p_{02} = p_{03} = 1.92$ one would predict based on Baur's suggestion central oxygen-phosphorous bond to be of 1.59 Å and terminal as of 1.53 Å.

In general, the study of the pyrophosphate family has been undertaken to understand the relative contribution of various factors in determining the chemical bonding by imposing small changes in a basic structure, as changes in the ionic radii of cations.

Although all the pyrocompounds with the thortveitite structure feature a linear X-O1-X bond, (since the anion lies on a centre of symmetry in C2/m space group) they also show an anomalously high anisotropic thermal motion for the central oxygen atoms. This could arise either because of strong thermal vibrations of central oxygen atom, or due to a completely random arrangement of bent P-O1-P groups between two

or more centrosymmetrically related positions (all the α phases do have bent X$\diagup^{O}\diagdown$X bonds). So far, among compounds studied, positional disordering seems to be the cause for $Cu_2P_2O_7$ while for others it is not clear. Study of $Mn_2P_2O_7$ was undertaken to find out the nature of the disorder of the P-O1-P group, in the light of already known facts about other members. This problem was of added interest, since $Mn_2P_2O_7$ was known to be unique in not showing α-β phase transitions.

CHAPTER II

THE CRYSTAL STRUCTURE OF $Mn_2P_2O_7$

a) Methods of X-ray Structure Determination

In order to indicate the manner in which the present crystal structure was determined, it is necessary to make a brief survey of the standard methods used for x-ray structure determination, as well as to define the various terms that are used in the process.

An ideal crystal is composed of atoms, arranged on a lattice defined by three fundamental translation vectors $\vec{a}$, $\vec{b}$, $\vec{c}$ such that the atomic arrangement is exactly the same, in every respect, when viewed from any point $\vec{r}$ as when viewed from the point

$$\vec{r}' = \vec{r} + n_1\vec{a} + n_2\vec{b} + n_3\vec{c} \ .$$

n_1, n_2, n_3 are arbitrary integers and $\vec{a}$, $\vec{b}$, $\vec{c}$ are a set of vectors characteristic of the crystal. The set of points specified by the above equation for all values of the integers n_1, n_2, n_3 define a lattice. A lattice is a regular periodic arrangement of points in space, and a crystal structure is formed only when a 'basis' of atoms is attached identically to each lattice point. When a parallel beam of x-rays is incident on such a crystal, it interacts with the constituent electrons of the atoms and coherent radiation will exit from

the crystal in well defined directions. If $\vec{a}$, $\vec{b}$, $\vec{c}$ are the vectors defining the repetitive unit or 'unit cell' of a crystal, and $\vec{k}$, $\vec{k}'$ are respectively wavevectors of incident and scattered x-rays, then these directions are such that they satisfy the Laue's condition

$$\underline{a}\cdot\underline{\Delta k} = 2\pi h$$

$$\underline{b}\cdot\underline{\Delta k} = 2\pi k$$

$$\underline{c}\cdot\underline{\Delta k} = 2\pi \ell$$

where $$\underline{\Delta k} = \underline{k} - k'.$$

Corresponding to the direct lattice vectors, $\vec{a}$, $\vec{b}$, $\vec{c}$ there exist three vectors $\vec{a}^*$, $\vec{b}^*$, $\vec{c}^*$ in reciprocal space such that

$$\vec{a}^* = \frac{\vec{b}\times\vec{c}}{V} \quad \vec{b}^* = \frac{\vec{c}\times\vec{a}}{V} \quad \vec{c}^* = \frac{\vec{a}\times\vec{b}}{V}$$

where $V = \vec{a}\cdot\vec{b}\times\vec{c}$ is the volume of the unit cell. Each point in reciprocal space is related to the direction of one of the diffracted x-ray beams and represents a set of planes of the direct lattice. In terms of a reciprocal lattice vector

$$\vec{H}(hk\ell) \equiv \vec{H} = ha^* + kb^* + \ell c^*$$

where h, k, ℓ are rigorously integers for an infinite crystal. The Laue conditions amount to

$$\Delta\vec{k} = \vec{H}.$$

A unit cell is not necessarily the smallest repetitive unit (primitive) of the atomic array, and is chosen with the view

of bringing out the symmetry of the crystal.

The intensity of the x-ray beam in different allowed directions, depends upon the arrangement of atoms within the unit cell. The observed intensity $I(hk\ell)$ of the reflection $(hk\ell)$ is, however, dependent upon a number of additional factors.

$I(hk\ell)$ may be written as

$$I(hk\ell) = K \cdot (L) \cdot (p) \cdot (A) \cdot |F(hk\ell)|^2$$

We will very briefly discuss each of the factors affecting intensity, other than the temperature factor, which is contained in this expression, because of its special importance for the problem at hand.

K, is an experimental constant, which depends upon the volume and density of the crystal, being exposed to the x-ray beam, the intensity of incident beam, efficiency of detection method (film or counter method).

The second factor is called the Lorentz factor, which is a geometrical factor, dependent upon the orientation of the incident and diffracted beam relative to the axis of rotation of the crystal. This leads to a dependence on θ, the angle of incidence, the exact functional form being decided by the recording technique.

The third factor is the polarization factor and arises because of the unpolarized incident x-ray beam, and varies with θ as $\frac{1}{2}(1+\cos^2 2\theta)$. The Lorentz and polarization factor

combined together are called the Lp factor.

The fourth factor is the absorption factor and as usual with electromagnetic radiation there is an exponential decrease in the intensity of x-ray beam as it travels through the sample. If I_o is the incident intensity, and μ is the linear absorption coefficient of the sample, then the intensity after traversing a distance x would be $I(x) = I_o \exp(-\mu x)$. The measured intensity must be corrected for the absorption and the correction depends upon the geometry of the crystal. Other than these factors,primary and secondary extinctions also affect the intensity, though not significantly except for very strong reflections.

The last and most important factor, which determines the distribution of the intensity of diffracted beam, is the structure factor F(H). The structure factor depends upon the way in which constituent atoms are arranged within the unit cell, and hence can be written as a function of the positions of the atoms within a unit cell. If there are N atoms in the unit cell, then the structure factor for the unit cell for the diffraction direction (hkℓ) is written as

$$F(H) = F(hk\ell) = \sum_{j=1}^{N} f_j \exp(-2\pi i \vec{H}\cdot\vec{r}_j)$$

where $\vec{r}_j$ is the position vector of the jth atom, f_j is the atomic scattering factor of the jth atom, and $\vec{H}$ is the reciprocal lattice vector as defined earlier, $\vec{H} = h\vec{a}^* + k\vec{b}^* + \ell\vec{c}^*$.

So far we have assumed that a crystal is a collection of

atoms, located at fixed points in the lattice. Actually the atoms do undergo thermal vibrations about their mean positions, at all the temperatures and the amplitude of vibration increases as the temperature increases. Thermal vibrations have the effect of decreasing the intensity of diffracted beam because of the smearing out of the lattice planes. The intensity of the diffracted beam decreases with an increase of temperature and at a particular temperature it causes a greater decrease in reflected intensity at high angles, conversely, at low temperature, it is the high angle reflections that show a marked increase in the intensity, as compared to their intensities at, say, room temperature.

Since the atomic scattering factor f_j, referred to above, is for atoms at rest, the expression for the structure factor must be modified to take into account the effect of thermal vibration. If, for simplicity one assumes that the displacement vectors $\vec{u}_j$ have an equal probability distribution in space, an assumption of vibrational isotropy, it can be shown that the overall result of the thermal motion of atoms is effectively to modify their scattering factors to

$$f_j^T = f_j^o \exp[-2\pi^2 \overline{(\vec{H}\cdot\vec{u}_j)^2}] \ .$$

If one represents the mean square displacement of the atom perpendicular to reflecting planes as $\overline{u_{\perp j}^2}$, above equation can be written as

$$f_j^T = f_j^o \exp[-B_j \sin^2\theta/\lambda^2]$$

where $B_j = 8\pi^2 \overline{u_\perp^2}$; (Woolfson, 1970)

and B_j is known as the temperature factor of the jth atom. Under the assumption of isotropic thermal vibrations, the value of B would be the same for all atoms, and hence we have

$$F^T_{hk\ell} = F^o_{hk\ell} \exp[-B \sin^2\theta/\lambda^2]$$

and for the intensity

$$I^T_{hk\ell} = I^o_{hk\ell} \exp[-2B \sin^2\theta/\lambda^2]$$

The factor, $\exp[-2B \sin^2\theta/\lambda^2]$, by which observed intensities are reduced is known as the Debye Waller factor

Although, in the early stages of structure determination it is sufficient to take the temperature factor to be isotropic and the same for all the atoms, in general it is rarely so and the magnitude and mode of vibrations of atoms differ depending upon their chemical environment. For example, since by and large, less energy is involved in changing bond angles than bond length, a terminal atom will tend to vibrate mainly in the directions perpendicular to the bond. If the second order tensor $\underline{\underline{u}}_j$ describes the anisotropic motion of the jth atom, the atomic scattering factor is modified as

$$f^T_j = f^o_j \exp(-2\pi^2 \vec{H} \cdot \underline{\underline{u}}_j \cdot \vec{H})$$

$$= f^o_j \exp[-2\pi^2 (u^c_{11}(ha^*)^2 + (u^c_{12}+u^c_{21})(ha^*kb^*) + \ldots.]$$

where subscript c is used to emphasize that the crystallographic axes are being used. u^c_{11} etc. are elements of a symmetric

tensor and form a matrix

$$u^c = \begin{pmatrix} u^c_{11} & u^c_{12} & u^c_{13} \\ u^c_{21} & u^c_{22} & u^c_{23} \\ u^c_{31} & u^c_{32} & u^c_{33} \end{pmatrix}$$

The square root of the component u_{ij} of $\bar{\bar{u}}$ gives directly the average root mean square displacement of an atom in the direction i. In general, the principal axes of the ellipsoid of thermal vibration bear no particular relationship to the crystallographic axes, these directions being determined by forces on an atom. Symmetry may,however,impose some restrictions. For example, if the atom lies on a two fold axis, one of the axes of ellipsoid must coincide with this axis. By diagonalising the above matrix, one can find the actual directions of three principal axes of the ellipsoid with respect to the crystallographic axes, as well as RMS amplitude along these axes.

The intensity of diffracted beam is recorded on a film or a diffractometer could be used for recording it. On a film, the darkening of spot is proportional to the intensity of reflection. It is convenient to record on a film only those reflections that belong to a plane in reciprocal space, such that out of the miller indices h,k,ℓ one is constant throughout. If the constant indices has value n, the reflections of that film are said to belong to nth layer.

The quantity by which one estimates the extent to which

the trial positions of atoms are correct, is the so called 'reliability factor' R. Assuming a normal distribution of errors in the observed structure factor $F_o(H)$ one assigns a weight $\omega(H)$ to the reflection (H), and then to get a best value of the positional and thermal displacement parameters of the atoms, one minimizes this 'weighted reliability factor' R_2 defined as

$$R_2^2 = \frac{\sum_H \omega(H)\,||F_o(H)|-|F_c(H)||^2}{\sum_H \omega(H)\,|F_o(H)|^2}$$

However, till the structure is known approximately one usually assigns unit weight to every observed reflection, and reliability is judged by 'unweighted reliability factor' R_1 defined as

$$R_1 = \frac{\sum_H ||F_o(H)|-|F_c(H)||}{\sum_H |F_o(H)|}$$

The systematic procedure by which R_2 is minimized is the so called 'Least Square Analysis'. If say, we have an error free set of $|F_o|$'s and an 'almost correct' set of atomic coordinates and temperature factors $(\vec{r}_j, \vec{B}_j)$ for the jth atom, then the 'correct' set of atomic coordinates and temperature factors $(\vec{r}_j+\Delta\vec{r}_j,\ \vec{B}_j+\Delta\vec{B}_j)$ are obtained by solving a set of equations, produced for each reflection

$$\Delta F_{hk\ell} = (F_o)_{hk\ell} - (F_c)_{hk\ell} = \sum_{j=1}^{N/2} \frac{\partial (F_c)_{hk\ell}}{\partial B_j} \Delta B_j + \overrightarrow{\nabla (F_c)}_{hk\ell} \cdot \overrightarrow{\Delta r}_j \quad -(A)$$

where for simplicity, isotropic temperature factors and a

centrosymmetric structure is assumed. In general, there are many more equations than parameters. These equations are truncated so as to be linear in the corrections to be made to the parameters and ideally, if a subset of these equations was taken such that the number of equations equalled the number of parameters then the correct parameters could be found and recalculated values of the F_c's would then equal the F_o's. However in practice the $|F_o|$'s are not error-free and so one finds a least square solution of a modified set of equations obtained by multiplying each equation of set (A) by an appropriate weight ω, according to the expected reliability of the quantity ΔF. The solution is one such that when the parameters are changed to $(B_j+\Delta B_j,\ r_j+\Delta r_j)$ the quantity

$$R_{sw} = \Sigma\ w|(F_o)-(F_c)|^2$$

is minimized. Many weighting schemes have been proposed and one used in this thesis is suggested by Cruickshank et al. (1961). This scheme uses $w = (A+B|F_o|+ C|F_o|^2)^{-1}$ where $A \simeq 2\ F_{min}$, $B = 1$, $C \simeq 2\ F_{max}$ and F_{min}, F_{max} are the minimum and maximum observed intensities.

b) Experimental

The experimental portion of the research consists of the determination of the structure of $Mn_2P_2O_7$ at two temperatures. The room temperature study supplemented the data already collected on $Mn_2P_2O_7$. A second set of data on the crystal were collected at low temperature ($\sim$ 100°K). A comparison of the positional and thermal parameters at these two temperatures is expected to aid in analysing the source of the anomalous thermal parameters of the bridging oxygen atom.

Both sets of data were collected using a Buerger Precession Camera with Mo(Kα) radiation.

Crystals were grown from a melt of $Mn_2P_2O_7$ powder from K & K Laboratories. The powder was sealed in an evacuated Vycor tube and heated to about 50°C above the melting temperature and was cooled slowly until the temperature was about 900°C. The sample was then quenched.

A crystal of dimensions 0.10×0.08×0.04 mm^3 was glued to a glass fibre with its longest side parallel to the fibre, to collect data at room temperature. Integrated precession photographs of the type of hk0, hk1, hk2, h0ℓ, h1ℓ and h2ℓ were taken. The rather small size of the crystal made it necessary to take photographs for as long as twenty seven cycles. Intensities were measured using a double beam recording microdensitometer (Joyce-Loebl Ltd.). It was necessary to employ

all three wedges, medium dark and light to keep the peak heights of integrated spots within a suitable range. Intensities of the same reflections measured from photographs with differing number of cycles, and with different wedges, in the case of very weak, or rather strong reflections, was brought to the same scale by finding the average values of ratio by which they differ. Reflections belonging to different layers were given different scale constants. All this raw intensity data was then corrected for the Lorentz and polarization effects.

The linear absorption coefficient for $Mn_2P_2O_7$ is 60 cms^{-1} for Mo(Kα) radiation. The crystal can be taken as having cylindrical geometry, then μR would be 0.25, and it was not considered necessary to apply absorption corrections.

The intensity data, at low temperature, was collected from a crystal of dimensions $0.2\times0.08\times0.08$ mm^3. The crystal was attached to a glass fibre using epoxy resin (as the ordinary glue is likely to shatter at low temperature), with its longest side parallel to the length of the fibre.

The apparatus used to collect the intensity data at low temperature was a 'cooled gas system'. This system was constructed by Dr. A. Prakash of our group.

Figure II-1 is a schematic representation of the system. The nitrogen gas coming from a cylinder first passes through copper coil B, which is immersed in liquid

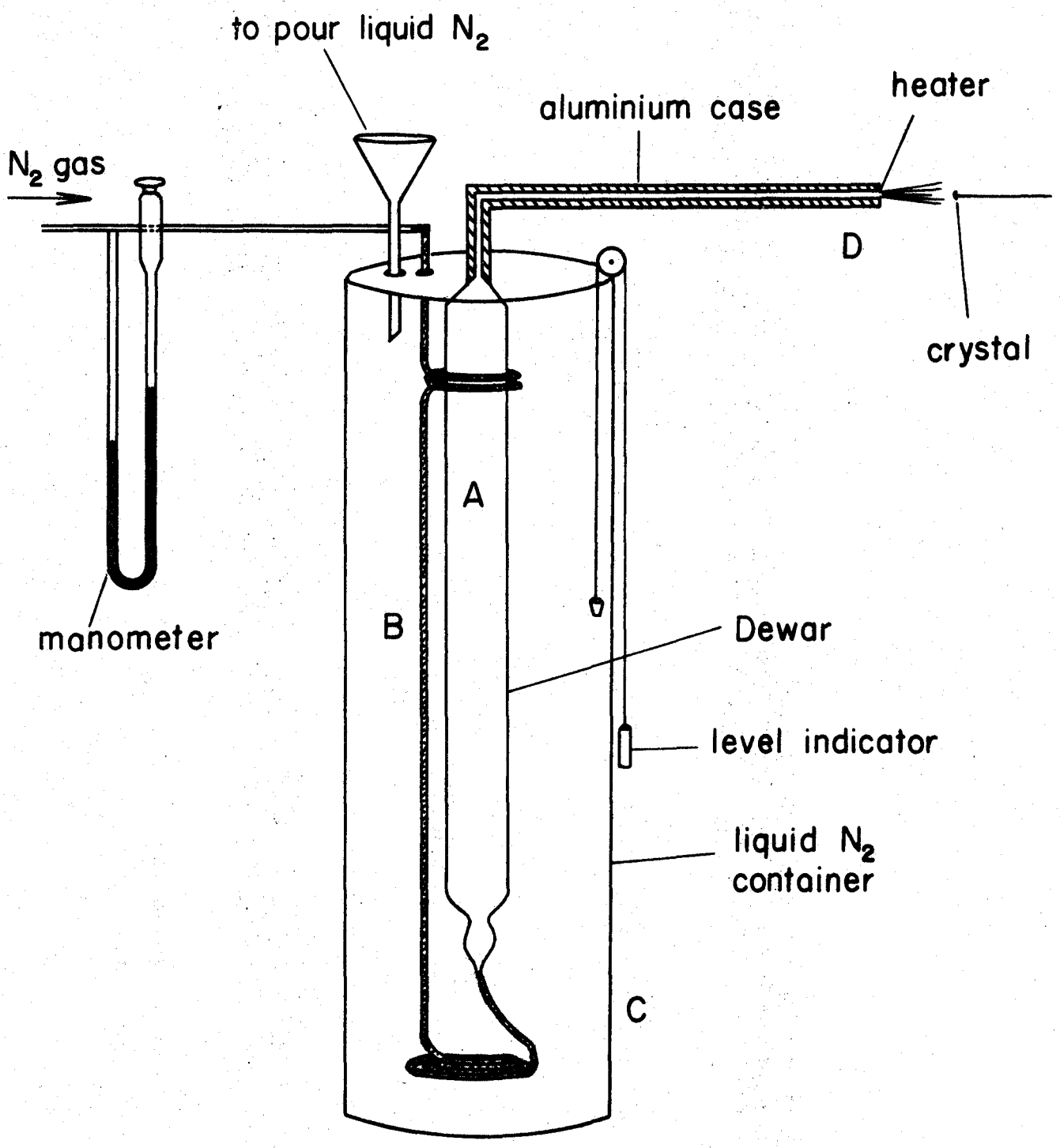

FIGURE II-1

The low temperature apparatus

nitrogen and then it passes through a double walled, internally silvered glass dewar flask A. The gas so cooled is impinged on the crystal. Liquid nitrogen is contained in a metallic dewar* C. The pressure of nitrogen gas is measured with a mercury manometer. The upper part of the copper coil is not immersed in the liquid nitrogen, however, the liquid nitrogen vapours serve to cool the incoming gas to some extent. The glass dewar A extends right through the metallic dewar C to the vicinity of crystal. The part of the dewar outside C is protected by an aluminum cover and can be rotated to some extent to adjust the position of the nitrogen stream with respect to the crystal. The dewar flask A is connected to the copper coils with a teflon tubing, in order to avoid the dewar cracking in case of accidental jerking of the system. Liquid nitrogen is poured in C through a hole at its top and its level is indicated by a simple device consisting of a string going over a pulley with inside end attached to a cork, which floats on the surface of liquid nitrogen, and outside end to a weight. A heater is attached to the D end of the Dewar to avoid frosting. A pressure of $\sim$ 15 mm of Hg was found to be enough to get well formed stream of nitrogen gas. The consumption of liquid nitrogen is approximately half a litre per hour for this pressure of nitrogen gas, and a full gas cylinder lasts for about 8-10 hours.

*Supplied by Supairco, Newark, U.S.A.

The temperature of nitrogen gas stream at the crystal is found tc be -180°±5°C. In order to get reproducible results it is important that the crystal is put in the centre of the nitrogen stream, so that it remains at a uniform low temperature as it rotates.

Many problems were faced while using the apparatus to collect data. The most serious of them was the choking of the copper coil, which happens if water vapour is present or is able to get into the copper coil during the experiment. The precautions to be taken to avoid this are to keep the apparatus at slightly positive pressure when not in use. One must always have one full gas cylinder on standby, while using another. Obviously using extra dry nitrogen gas would be helpful. One should not be tempted to overfill the metallic dewar C with liquid nitrogen, which increases the chances of moisture getting into the system, and eventually choking it up. It is more than enough to fill it half, as consumption of liquid is very little. If, however, the apparatus does get choked, one must take out the glass dewar with copper coils from C carefully, pass air and then nitrogen gas for a sufficiently long time to ensure that no moisture is left inside. The position of the dewar arm must be adjusted as much as possible before pouring liquid nitrogen, as teflon gets hardened once put in liquid nitrogen and cracks if any twist is caused by way of adjusting the arm of the dewar. It was just not possible to carry out the experiment during many

humid days of summer, because of the fast growth rate of frost around the crystal. The x-ray picture shows scattered spots all over once there is any ice formation around the crystal. Although rapid flow of nitrogen gas helps, occasionally gentle blowing of air is necessary to prevent ice buildup, even when heater is working properly. If ice formation takes place, one must reduce the flow of nitrogen to the minimum to get the crystal to room temperature and then start all over again after checking the alignment of the crystal. The crystal may go off alignment by a few degrees whenever the crystal is brought to room temperature from low temperature, or vice versa. It was found to be most convenient to collect as much data as possible when the moisture contents happened to be lowest. The photographs could not be taken at precession angle of more than 25°, because of the obstruction by the dewar arm. Integrated photographs up to three cycles were taken for all the layers. As in the case of room temperature data, the intensity of integrated films was measured by recording microdensitometer, scaled properly and corrected for the Lorentz and polarization effects using PRELP programme. Since the dimensions of crystal were $0.2\times0.08\times0.08\ mm^3$ μR would be 0.25, and approximating it with a cylinder, it was considered to be not necessary to apply absorption corrections.

Lattice parameters at room temperature were obtained by a least squares fit of twenty-four lines of a Debye-Scherrer

photograph. The reflections used, together with their measured and calculated 'Theta(θ)' values, are shown in Table II-1. The low temperature lattice parameters were determined by taking superposed precession photographs of the crystal at low temperature and room temperature and finding the percentage change in the spacing of spots. The lattice parameters obtained are a = 6.620±0.001 Å, b = 8.578±0.002 Å, c = 4.538±0.001 Å, β = 102.80±0.05° at 23°C and a = 6.600±0.001 Å, b = 8.543±0.002 Å, c = 4.528±0.001 Å, β = 102.81±0.05 Å at -180°C. The lattice parameters of compounds known to be of thortveitite structure are given in Table II-2 for comparison.

c) Refinement and Results

The atomic positional and thermal parameters obtained by Dr. Calvo were used as the starting point for the refinement of structure of $Mn_2P_2O_7$ at room temperature. Anisotropic temperature factors for the Mn, P, 01 and the 02 atoms were non positive definite.

Room temperature

C2/m space group symmetry was used. 330 reflections of hk0, hkl, hk2 (zone 1) and 282 reflections of h0ℓ, hlℓ, h2ℓ type (zone 2), corrected for the Lorentz and polarization effects, were put to the least squares refinement, separately. Only scale constants were allowed to vary, and initially unit weights were assigned to all the reflections. Many strong reflections, which presumably were not measured accurately, being outside the limit of linearity range, were given zero weight. The agreement factors for zone 1 and zone 2 were respectively 0.199 and 0.242, after the scales were refined. Then, the scale constants as well as the positions of the atoms were allowed to vary. After a few cycles of refinement by least squares, reflections of zone 1 had an R_1 value of 0.09 and of zone 2 had R_1 value of 0.122.

Data of both the zones were combined and a cycle of least squares refinement was calculated varying the atomic coordinates, scale constants as well as the anisotropic temperature factors for all the atoms. R_1 values for all the

reflections was 0.100. The phosphorous atom and the 0-1 atom showed non-positive definite temperature factors.

At this stage, Cruickshank's weighting scheme was introduced to take into account the systematic errors inherent in measurements of integrated intensity. The functional form of the weighting curve and the values of constants used are given in Table II-3. The equivalent reflections were averaged and were put to one overall scale factor. Further cycles of refinement reduced R_1 to 0.064 and the weighted agreement factor R_2 was 0.084 (R_1 and R_2 have been defined earlier in the theory section). Only the phosphorous atom's temperature factor remained non-positive definite now.

The room temperature data collected by Dr. Calvo consisted of eight layers with overall R_2 of 0.13. This data were combined with the above data. Least squares refinement cycles were done to get the best value for their relative scale constants, after which equivalent reflections were averaged and then all the reflections were put to an overall scale factor. Further least squares refinement cycles were calculated until the values of R_1 and R_2 became practically constants and the parameters showed insignificant shift.

All the relevant data of room temperature refinement are in Table II-3. The magnitude of observed and calculated structure factors based on these final parameters are in Table II-4.

Low temperature (-180°C)

Here, again, the atomic positional and the temperature parameters of the partially refined structure of $Mn_2P_2O_7$ at room temperature were used as the initial trial structure. First only the scales of 564 reflections (including unobserved ones) belonging to two zones of the same crystal and corrected for the Lorentz and polarization effects, were refined. Unit weights were assigned to all the reflections and C2/m space group was used. For the first zone, the overall agreement factor, R_1, was 0.129, while for second R_1 was 0.117. But for the third layer of first zone for which R_1 was 0.235, the agreement factor for individual layers was close to the value of overall value of R_1. The reason for this was found to be rather inaccurate scaling of the reflections measured with different wedges. Hence in this case the intensities were estimated by visual comparison and the agreement factor for this layer came in line with the others.

Next the reflections of both the zones were put together and Cruickshank's weighting scheme was introduced. The values of the constants are given in Table II-5. A few cycles of least square refinement, varying the atomic coordinates and the anisotropic temperature factors of every atom along with the scale constants brought down R_1 value to 0.099. The weighted agreement factor R_2 was 0.116. It was only the O1 atom which showed non-positive definite temperature factor.

At this stage, the equivalent reflections were averaged

and all the reflections were put to same overall scale factor. Least squares refinement was carried out till R_1 and R_2 showed no appreciable change.

The final values of unweighted agreement factor R_1 was 0.072 and the R_2 was 0.101. All the atoms had positive definite temperature factors at this point.

All the relevant details of the low temperature refinement are given in Table II-5. The magnitude of observed and calculated structure factors based on final values of least square parameters are given in Table II-6.

The computer programme CUDLS was used for the refinement of the structure, throughout.

The refined atomic positional coordinates and the anisotropic thermal parameters at room temperature and low temperature are compared in Table II-7 and Table II-8. The diagonalised root mean square displacement (in Å) at room and low temperature and the direction cosines of the principal axes of the thermal ellipsoid with the crystal axes, are given in Table II-9.

TABLE II-1

Observed and calculated values of θ for the Debye-Scherrer lines used to determine the lattice parameters of $Mn_2P_2O_7$ at room temperature

h	k	ℓ	Theta (Obs.)	Theta (Calc.)
1	1	0	3.9750	3.9948
0	0	1	4.6250	4.6012
1	1	1	6.6125	6.5721
-2	0	1	6.9500	6.9501
2	2	0	7.8850	7.9084
2	0	1	8.6100	8.6015
1	-3	1	9.4600	9.4260
-3	1	1	9.8850	9.8922
0	4	1	10.5250	10.6065
-2	2	2	11.0850	11.0820
-1	-3	2	11.6000	11.5855
3	3	0	11.9750	11.9106
2	0	2	12.3500	12.3214
1	3	2	12.6875	12.6634
-1	5	1	13.0000	12.9737
-4	2	1	13.4625	13.4182
0	0	3	13.9250	13.9255
0	6	0	14.4125	14.3884
3	5	0	15.4125	15.3461
-2	6	1	16.0625	16.0448
-2	6	2	17.6100	17.6403
6	0	0	19.2875	19.2440
5	5	1	21.6125	21.5075
-1	5	4	22.0600	22.0664

TABLE II-2

Lattice parameters of structures of thortveitite class
(e.s.d.'s in parentheses)

	Ref.	a(Å)	b(Å)	c(Å)	β(°)
$Mn_2P_2O_7$ (23°C)	1	6.620(1)	8.578(2)	4.538(1)	102.80(5)
$Mn_2P_2O_7$ (-180°C)	1	6.600(1)	8.543(2)	4.528(1)	102.81(5)
β-$Cu_2P_2O_7$	2	6.827(6)	8.118(6)	4.567(6)	108.85(10)
β-$Mg_2P_2O_7$	3	6.494(7)	8.28 (1)	4.522(5)	103.8 (1)
β-$Zn_2P_2O_7$	4	6.61 (1)	8.30 (1)	4.51 (1)	105.4 (1)
β-$Ni_2P_2O_7$	5	6.501 (1)	8.239(1)	4.480(1)	104.14(1)
$Mg_2As_2O_7$	6	6.584	8.509	4.761	103.9
$Zn_2As_2O_7$	7	6.66	8.36	4.75	104.
$Cd_2V_2O_7$	8	7.088(5)	9.091(5)	4.963(5)	103.3 (5)
$Zn_2V_2O_7$	9	7.31	8.32	5.15	111.5
$Mn_2V_2O_7$	10	6.710(2)	8.726(2)	4.970(1)	103.57(1)
$Sc_2Si_2O_7$	11	6.542(5)	8.519(5)	4.669(5)	102.5(2)

References for Table II-2

1. Present work
2. B. E. Robertson and C. Calvo (1968)
3. C. Calvo (1965a)
4. C. Calvo (1965b)
5. A. Pietraszko and K. Lukaszewicz (1968)
6. K. Lukaszewicz (1963)
7. C. Calvo and Neelkantan (1967)
8. P.K.L. Au and C. Calvo (1967)
9. C. Calvo, Private communication
10. Ebba Dorm and Bengt-olov Marinder (1967)
11. D.W.J. Cruickshank, H. Lynton and G. A. Barclay (1962)

TABLE II-3

Room temperature (23°C) refinement data for $Mn_2P_2O_7$

$\mu(MoK\alpha) = 60\ cms^{-1}$

Number of observed reflections = 352

Total number of reflections = 459

Weighting curve $w = (A+B|F_o|+C|F_o|^2)^{-1}$

Weighting curve constants

A = 5.

B = 1.

C = 0.04

R_1 (observed reflections only)	0.088
R_1 (all reflections)	0.090
R_2 (observed reflections only)	0.117
R_2 (all reflections	0.120

Unobserved reflections whose calculated values were greater than the minimum observed value, F(min) in that area were replaced by 0.90 F(min), otherwise their weight was set at zero.

TABLE II-4

TABLE OF OBSERVED REFLECTIONS OF MN2P2O7 AT ROOM TEMPERATURE . UNOBSERVED

ARE MARKED WITH L

TABLE II-5

Low temperature (-180°C) refinement data for $Mn_2P_2O_7$

$\mu(MoK\alpha) = 60\ cms^{-1}$

Number of observed reflections = 253

Total number of reflections = 286

Weighting curve $w = (A+B|F_o|+C|F_o|^2)^{-1}$

Weighting curve constants

$A = 8.$

$B = 1.$

$C = 0.02$

R_1 (observed reflections only)	0.072
R_1 (all reflections)	0.072
R_2 (observed reflections only)	0.101
R_2 (all reflections)	0.101

Unobserved reflections whose calculated values were greater than the minimum observed values, F(min) in that area were replaced by 0.90 F(min). Otherwise their weight was set at zero.

TABLE II-6

TABLE OF OBSERVED REFLECTIONS OF MN2P2O7 AT LOW TEMPERATURE . UNOBSERVED

ARE MARKED WITH L

TABLE II-7

Atomic coordinates of $Mn_2P_2O_7$ (e.s.d.'s in par ntheses) at room temperature (23°C) and low temperature (-180°C)

The low temperature coordinates are given in brackets

Space group C2/m

	x/a	y/b	z/c
Mn	0	0.3096(2) {0.3090(2)}	1/2
P	0.2155(4) {0.2171(5)}	0	0.9092(5) {0.9094(6)}
01	0	0	0
02	0.3742(10) {0.3733(15)}	0	0.2082(14) {0.2041(18)}
03	0.2209(9) {0.2246(11)}	0.1489(8) {0.1476(8)}	0.7258(13) {0.7277(14)}

TABLE II-8

Thermal coordinates (in $\mathring{A}^2$) of $Mn_2P_2O_7$ at room temperature (23°C) and low temperature (-180°C) (e.s.d.'s are in parentheses and low temperature values are in brackets)

	U_{11}	U_{22}	U_{33}	U_{12}	U_{13}	U_{23}
Mn	0.0061(8)	0.021(1)	0.0143(7)	-	0.0045(5)	-
	{0.011 (1)}	{0.007(1)}	{0.0131(1)}	-	{0.0016(7)}	-
P	*0.004 (1)	0.020(2)	0.0094(9)	-	0.0061(7)	-
	{0.004 (2)}	{0.007(2)}	{0.010 (1)}	-	0.001 (1)	-
01	0.008 (5)	0.064(12)	0.024 (6)	-	0.012 (5)	-
	{0.003 (7)}	{0.032(1)}	{0.038 (8)}	-	{0.010 (6)}	-
02	0.004 (2)	0.007(3)	0.009 (2)	-	0.004 (2)	-
	{0.012 (5)}	{0.013(5)}	{0.009 (3)}	-	-0.004 (3)	-
03	0.007 (2)	0.025(3)	0.017 (2)	0.003(2)	0.004 (2)	0.004(2)
	{0.014 (4)}	{0.004(4)}	{0.019 (3)}	{0.003(2)}	{0.0004(27)}	{-0.003(2)}

*Non positive definite

TABLE II-9

Diagonalized root mean square thermal vibrations for $Mn_2P_2O_7$ at room temperature and low temperature

	-180°C				23°C			
	RMSA(Å)	Direction Cosines*			RMSA(Å)	Direction Cosines		
Mn	0.119	0.591	0.00	-0.017	0.145	0.000	1.00	0.000
	0.106	0.807	0.00	0.399	0.120	-0.151	0.0	-0.931
	0.086	0.0	1.0	0.0	0.069	0.989	0.0	-0.365
P	0.102	0.171	0.0	-0.999	0.141	0.0	1.0	0.0
	0.085	0	1.0	0.0	0.106	-0.390	0.0	-0.812
	0.068	0.961	0.0	-0.05	-	-	-	-
01	0.195	0.071	0.0	0.957	0.253	0.0	1.0	0.0
	0.179	0	1.0	0.0	0.174	-0.240	0.0	-0.894
	0.033	0.998	0.0	-0.289	0.056	0.971	0.0	-0.448
02	0.136	-0.836	0.0	0.720	0.100	0.298	0.0	0.866
	0.114	0	1.0	0.0	0.086	0.0	1.0	0.0
	0.077	-0.549	0.0	-0.694	0.038	0.955	0	-0.501
03	0.155	-0.632	0.225	0.863	0.163	0.106	0.992	0.340
	0.110	0.741	0.104	0.483	0.126	-0.013	-0.374	0.908
	0.058	0.226	-0.969	-0.148	0.075	0.994	-0.103	-0.246

*Direction cosines defined along the crystallographic directions

CHAPTER III

DISCUSSION AND CONCLUSION

Łukaszewicz and Smajkiewicz (1961) first reported the crystal structure of $Mn_2P_2O_7$. They concluded that its structure is of the thortveitite type, using 72 observed structure factors for two projections. Although the R value obtained was around 0.18, the reported phosphorous-oxygen bond distances did not appear to be realistic. The two symmetry independent non bridging P-O bond lengths were 1.74 Å and 1.60 Å, while for example in β-$Zn_2P_2O_7$, these lengths are 1.556 Å and 1.554 Å and for β-$Mg_2P_2O_7$ they are 1.534 Å and 1.542 Å. No crystallographic evidence of a phase transition has been observed in $Mn_2P_2O_7$. Lazarev (1962) studied infrared absorption at temperatures as low as -150°C did not find any noticeable change in the spectrum for this crystal.

First we shall discuss the details of the refined structure of $Mn_2P_2O_7$ as such in particular, then we shall compare the small differences between β (high temperature phase) structure of the various other compounds of this series with that of $Mn_2P_2O_7$. The points of interest in comparison would be the nature of the differences in the distortion of the environment of the cation, the agreement with the predicted bond lengths by Cruickshank and by Baur, the differences

in the positional and thermal coordinates of $Mn_2P_2O_7$ itself at 23°C and -180°C and finally the anomalous anisotropic thermal parameter for the central oxygen atom in $Mn_2P_2O_7$ and other members in the series.

$Mn_2P_2O_7$ has space group C2/m, with two molecules per unit cell and hence has four equivalent manganese, four phosphorous atoms and fourteen oxygen atoms in a unit cell. Apart from one type oxygen atom which could be in a general position, the rest should be all in special positions.

The geometrical features of both the pyrophosphates anion and manganese-oxygen polyhedron as seen in a-c projection is shown in Figure III-1 and tabulated in Table III-1.

Each phosphorous atom in the pyrophosphate anion is situated on a mirror plane (a-c plane) which is perpendicular to the b axis, and is bonded to four oxygen ions. The central oxygen atom shared by the two phosphate tetrahedra is labelled 01, the terminal oxygen of each of the PO_4 tetrahedra lying on the mirror plane is labelled 02. The two phosphorous atoms are symmetry related by means of the two fold axis passing through 01, so that bond angle P-01-P is linear. Each of the remaining pairs of oxygen atoms related by the mirror plane are labelled 03. The two phosphate tetrahedra are thus forced in a staggered configuration, when viewed along the P-P vector.

Each of the terminal oxygen atoms 02 and 03 are bonded

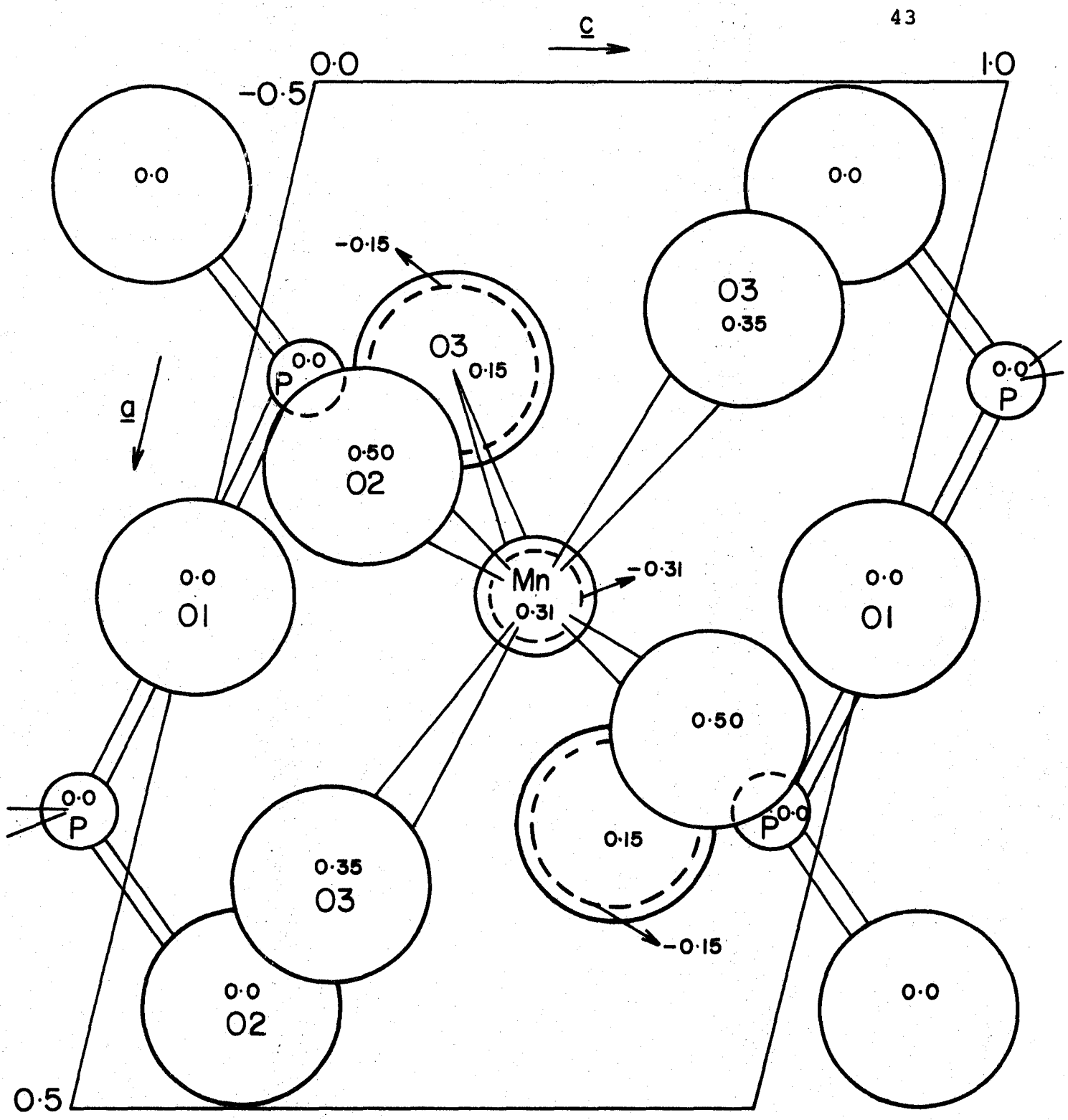

FIGURE III-1

Geometry of cation and anion in $Mn_2P_2O_7$

to three atoms: the phosphorous atom and two manganese atoms. The phosphorous atom is tetrahedrally coordinated to the central oxygen and the terminal oxygen atoms in the anion. The bond angles O1-P-O2, O1-P-O3, O2-P-O3 and O3-P-O3 are 104.6(3)°, 106.0(3)°, 113.0(3)° and 113.3(5)° respectively*. They are close to the tetrahedral angle of 109°28' though still significantly different. The values of bond lengths P-O1, P-O2 and P-O3 are 1.570(3)Å, 1.521(6)Å and 1.529(7)Å with e.s.d.'s given in the parentheses.

Each of the manganese ions is sixfold coordinated to the neighboring oxygen ions in a distorted octahedron. The two fold axis passes through manganese and hence three of the oxygen atoms would generate all the oxygen atoms of the octahedron. The three unique manganese-oxygen bond distances are: Mn-O2 of 2.150(4)Å and two of Mn-O3(a) and Mn-O3(f) as of 2.104(6)Å and 2.330(6)Å respectively. Each of the manganese oxygen octahedron shares three edges with the neighbouring manganese atoms. Two of these edges are related by the two-fold axis and are of shorter length, 2.554(10)Å, than the remaining one of length 2.799(8)Å which is in the mirror plane. This is shown diagramatically in Figure III-2, which is a projection of $Mn_2P_2O_7$ on the a-b plane. The manganese atoms form sheets of distorted hexagonal network, and the anions lie on the centres of these distorted manganese hexagons, with the central oxygen atom O1 midway between the sheets of man-

*Values at 23°C.

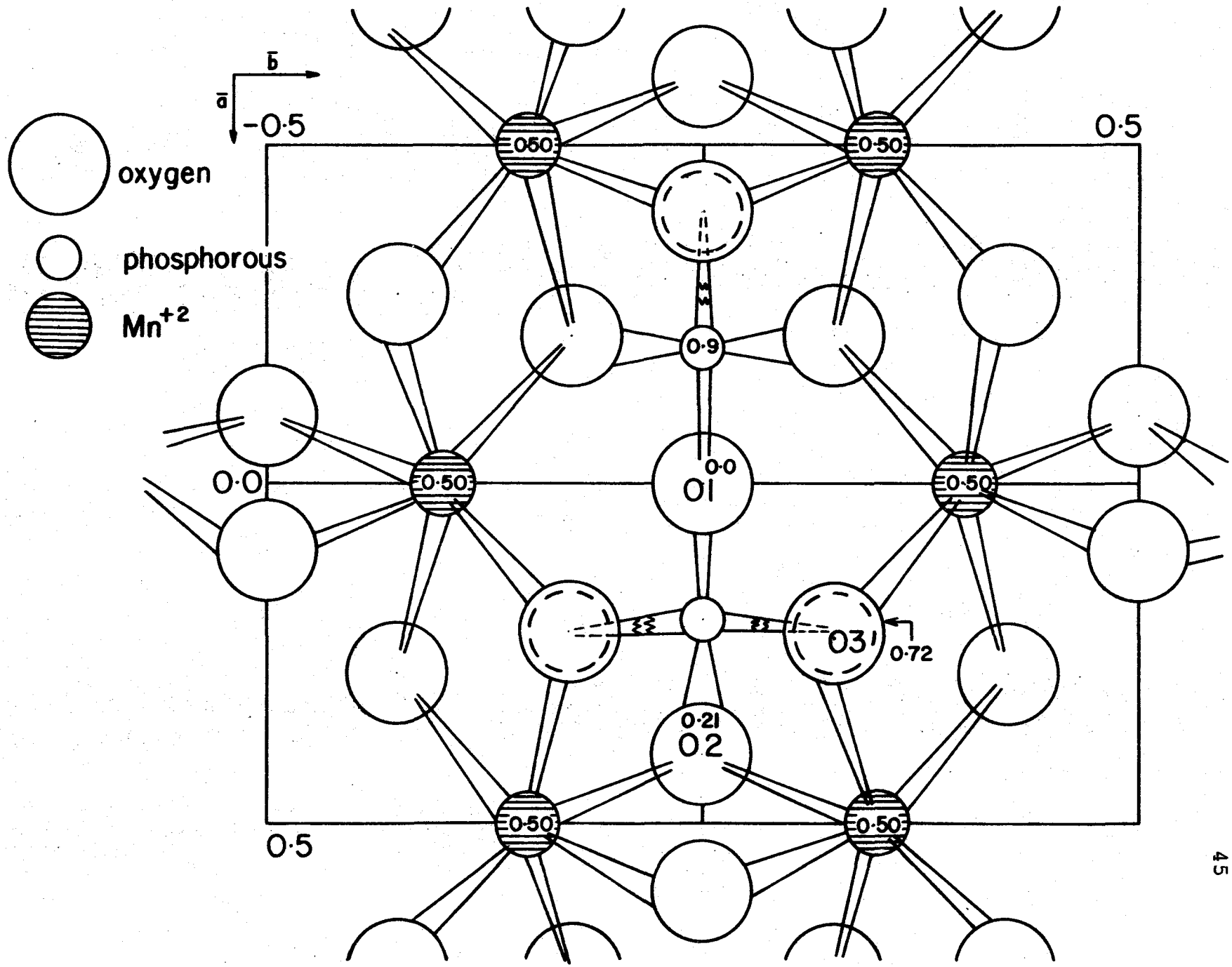

FIGURE III-2 Hexagonal arrangement of Mn^{+2} layer in $Mn_2P_2O_7$ (C2/m space group)

ganese. The anions thus form a link between these sheets through the terminal oxygens of the pyrophosphate anion.

The important bond lengths and interatomic angles of the structures of β-$Mg_2P_2O_7$, β-$Zn_2P_2O_7$ and β-$Cu_2P_2O_7$ are compared with those of $Mn_2P_2O_7$ in Table III-2. Looking at X-O bond lengths, one notices that one of the three is always significantly longer than the other two. This is typical of the distortion of the octahedral environment of the cations in the β phase, that they show longer axial cation-oxygen bonds X-O3(f) than equatorial bonds and it is due to the non-spherical P-O-P groups in the empty octahedral site. For $Mn_2P_2O_7$ the axial bond length is 2.3 Å and the equatorial average is 2.1 Å. The case of extreme distortion is however β-$Cu_2P_2O_7$ (Robertson and Calvo, 1968) where the axial bond length is of 2.58 Å as compared to an average equatorial bond length of 1.9 Å, with the result that P-O1 bonds parallel to Cu-O3(f) are unusually shortened.

All of the P-O(-P) bond lengths of compounds listed in Table III-2 are shorter than their predicted value by Cruickshank, and these are short by 0.01 Å for $Mn_2P_2O_7$ and 0.04 Å for β-$Cu_2P_2O_7$. The predicted values (see Chapter I) by Cruickshank for a linear P-O1-P group is 1.58 Å and 1.53 Å for P-O bond length. Since Cruickshank assumed an isolated $P_2O_7^{4-}$ ion, all the external bonds were considered equivalent. The predicted bond lengths are dependent upon amount of pπ-dπ

bonding within the anion, which could change when an isolated anion is put in a crystalline environment. In Table III-3, the three angles subtended, at each independent terminal oxygen atom by its three ligands, is given for some of the β structure compounds, along with those in $Mn_2P_2O_7$. In each case, the sum of angles total to approximately 360°, which implies that the mean positions of 02 and 03 lie very nearly in the same plane as the two cations and phosphorous atoms to which they are bonded (Robertson and Calvo, 1967).The terminal oxygen atom would then be expected to have some sp^2 character, which would of course change the amount of dπ-pπ bonding within the anion (Stager and Atkinson, 1969). Moreover, the experimental bond lengths are not necessarily the true time averaged bond lengths because of the large component of thermal motion for 01 atoms. In order to make the proper correction, it is necessary to know the manner in which the motion of the 01 atom is correlated with the motion of P atoms. A proposed correction, which does not take into account the exact details of the motion but gives the minimum correction (Busing and Levy, 1964) when applied to P-O-P distance in β-$Cu_2P_2O_7$ increases it to 1.564 Å from its uncorrected value of 1.542 Å (Robertson, 1967). Thus, the effect of the environment and nonlinearity of P-01-P bond appears to be the cause of the deviation from predicted values of bond lengths.

One could also compare the experimental values for

for the P-O-(-P) and terminal P-O bond lengths, with that predicted by Baur, as discussed in Chapter I. The predictions are 1.59 Å for the central and 1.53 Å for terminal P-O bonds. Thus, the prediction for the terminal bond is the same as that of Cruickshank but Baur predicts a larger bond length for the central phosphorous-oxygen bond. Since the prediction is correct only within an accuracy of about 0.02 Å, both the observed bond lengths P-O1(-P) of 1.570 Å and the average P-O bond length of 1.525 Å at 23°C for $Mn_2P_2O_7$ lies well within the reliability, so also are the bond lengths for Zn^{+2}. The apparent difference in P-O bond length of Mg^{+2} from the predicted value may not be significant because of the large errors associated with the experimental result. As suggested by Baur, in general, the reasons for a significant deviation from the predicted value assuming the model of the structures to be correct and the bond lengths to be accurate could be second neighbour interactions and the influence of shared edges.

For $Mn_2P_2O_7$, the atomic positional coordinates at 23°C and -180°C are compared in Table II-7, while the molecular bond geometry is compared in Table III-1. The rather significant change in the x coordinate of P atom, and so also of O3 atom, as well as slight changes in the bond angles O1-P-O3 may be taken to indicate a decreased thermal motion of the atoms.

Looking at the anisotropic thermal parameters for $Mn_2P_2O_7$ (Table II-8) it is only for the P atom at room temperature that one has non positive definite temperature factor, implying that the P atom at room temperature can not be represented by an ellipsoid for its thermal motion.

A feature common to all the thortveitite compounds is that the central oxygen atom 01, shows an anomalously high anisotropic temperature factor. The largest component of thermal vibration is perpendicular to P-P vector and is in the direction of b axes (component U_{22}). Since this indicates that P-01-P bond is essentially non-linear, associated with this common feature is the problem that whether this motion is real or represents a statistical positional disordering, and if real whether it represents a rotational or vibrational thermal motion.

If one compares the R.M.S. amplitude of the vibration of $Mn_2P_2O_7$ at room temperature with that at low temperature (Table II-9), it is clear that the only significant change that has occurred is in the amplitude of vibration of the 01 atom in the b direction, this direction because of symmetry must always be one of the principal axes of the thermal ellipsoid.The R.M.S.amplitude has reduced from 0.25 Å to 0.18 Å . One must expect because of this a change in P-01 bond length. However, there is no significant change

observed.

For all the atoms, except 02, the rms amplitude of vibration is decreased, in going from the room temperature to the low temperature. The opposite trend for the 02 atom could be because the thermal motions of P and 02 are interdependent and the thermal parameter for the P atom shows non positive definite at room temperature. Moreover, since there is comparatively less data at low temperature, scale constants could also affect the temperature factor, and one would tend not to look for any physical reasoning for this anomaly.

Another interesting observation is the change in the direction of the vibration of maximum amplitude (major axis of the ellipsoid) in going to the low temperature. For all the atoms in special position Mn, P, 01 and approximately for the 02 atom, the major axis is along the b axis, at room temperature. At low temperature, for Mn atoms, the b axis becomes the direction of the minimum amplitude of vibration, and also for P, 01 and 02 atoms it is only one of the minor axes of the ellipsoid. It is difficult to say whether or not this indicates a significant change in the motion.

In Table III-4 the R.M.S. amplitudes of the vibration and the direction cosines for the thermal ellipsoids of β-$Cu_2P_2O_7$ and $Cd_2V_2O_7$ (which have β structure) have been tabulated. A comparison of these two compounds with $Mn_2P_2O_7$ at room temperature shows that while for β-$Cu_2P_2O_7$ the major

axis of thermal ellipsoid of O-1 and P atom is in the direction of the b axis as for $Mn_2P_2O_7$, it is not the case for $Cd_2V_2O_7$. While for the cations, the direction of the major axis is different in all three compounds, it is the same and is the b direction for the P, V and 02 atom. Since all the three compounds have the same structure, one would expect that they should have similar directions, as directions of the maximum thermal vibration and maybe this arbitrariness is because they do not represent averages of the thermal motion.

There have been attempts to see if the structure could be better represented by considering a random distribution of the bridging oxygen on two positions, one on each side of the origin (Ebba Dorm et al, 1967) but resulted in no significant improvement.

To conclude, although it appears that by going to low temperature, β phase of $Mn_2P_2O_7$ is getting more stabilised as the thermal motion is more isotropic and better represented by thermal ellipsoids, there is no way one could decidedly say as to what is the source of anomaly. Among the compounds studied, it is only for $Cu_2P_2O_7$ (Calvo and Robertson, 1967) that it was concluded that this anomalous motion is due to the positional disordering, while for others, the problem remains as it is.

Hopefully, by collecting x-ray data at the liquid helium temperature for $Mn_2P_2O_7$, one would be in a position to decide this, and is proposed to be done as soon as possible.

TABLE III-1

Molecular geometry of $Mn_2P_2O_7$ at -180°C and 23°C
(e.s.d.'s in parentheses)

a) Bond Lengths (Å)

	-180°C	23°C
Mn-02	2.159(5)	2.150(4)
Mn-03(a)	2.117(7)	2.104(6)
Mn-03(f)	2.310(8)	2.330(6)
P-01	1.574(3)	1.570(3)
P-02	1.495(8)	1.521(6)
P-03	1.513(7)	1.529(7)
01-02	2.432(9)	2.448(6)
01-03	2.473(8)	2.475(7)
02-03	2.504(9)	2.544(8)
03-03(b)	2.522(10)	2.554(10)

b) Bond Angles (°)

02(e)-Mn-03(f)	85.4(3)	85.3(2)
-03(a)	158.0(3)	158.4(3)
-02(g)	81.8(2)	81.2(2)
-03(d)	93.3(2)	93.7(2)
-03(g)	80.6(3)	81.4(2)
03(f)-Mn-03(a)	115.0(3)	114.8(2)
-02(g)	80.6(3)	81.4(3)
-03(d)	77.7(2)	77.3(2)
-03(g)	161.5(3)	162.4(3)

(continued next page)

TABLE III-1 (continued)

	-180°C	23°C
03(a)-Mn-03(d)	98.7(3)	98.1(3)
01-P-02	104.8(5)	104.7(3)
-03	106.5(3)	106.0(3)
02-P-03	112.7(4)	113.0(3)
03-P-03(b)	112.9(5)	113.3(5)

Note: The alphabets used denote equivalent positions of atoms as follows:

a ≡ x, y, z;

b ≡ $x, \bar{y}, z$;

c ≡ $\bar{x}, \bar{y}, \bar{z}$;

d ≡ $\bar{x}, y, \bar{z}$;

e ≡ $x+\frac{1}{2}, y+\frac{1}{2}, z$;

f ≡ $x+\frac{1}{2}, \bar{y}+\frac{1}{2}, z$;

g ≡ $\bar{x}+\frac{1}{2}, \bar{y}+\frac{1}{2}, z$;

h ≡ $\bar{x}+\frac{1}{2}, y+\frac{1}{2}, \bar{z}$;

TABLE III-2

Molecular geometry of the high temperature form (β) of compounds of type $X_2P_2O_7$
(e.s.d.'s in parentheses)

(a) Bond lengths (Å)

X	Mn^{+2}	Mg^{+2}	Zn^{+2}	Cu^{+2}
X-02	2.150(4)	2.05	2.061	2.003(15)
X-03(a)	2.104(6)	2.02	2.001	1.936(15)
X-03(f)	2.330(6)	2.15	2.275	2.577(15)
P-O(1)	1.570(3)	1.557(2)	1.569(5)	1.542(4)
P-O(2)	1.521(6)	1.534(10)	1.556(19)	1.516(15)
P-O(3)	1.529(7)	1.542(9)	1.554(13)	1.503(15)

(b) Angles

O(1)-P-O(2)	104.7(3)°	103.3°	102.1°	105.5°
-O(3)	106.0(3)°	106.8°	110.0°	108.7°
O(2)-P-O(3)	113.0(3)°	113.3°	110.9°	111.0°
O(3)-P-O(3)	113.3(5)°	112.6°	112.6°	111.8°

Note the alphabets a, f, stand for a particular equivalent position of atom, as defined in Table III-1.

TABLE III-3

Sum of angles subtended at the terminal oxygen atoms of the pyroanion in the high temperature form of some compounds of the type $X_2Y_2O_7$

a) $Mn_2P_2O_7$

P-O2-Mn1(e)	130.24°	P-O3-Mn1(f)	118.91°
-Mn1(b)	130.24°	-Mn	135.63°
Mn-O2-Mn	98.81°	Mn-O3-Mn1(f)	102.66°
	359.29°		357.20°

b) β-$Cu_2P_2O_7$

P-O2-Cu1(e)	129.6°	P-O3-Cu1(f)	118.1°
-Cu1(b)	129.6°	-Cu	135.6°
Cu-O2-Cu	99.8°	Cu-O3-Cu1(f)	103.2°
	359.0°		356.9°

c) $Cd_2V_2O_7$

V-O2-Cd1(e)	129.03°	V-O3-Cd1(f)	120.55°
-Cd1(b)	129.03°	-Cd	129.93°
Cd-O2-Cd	100.42°	Cd-O3-Cd1(f)	105.49°
	358.48°		355.97°

Note: The alphabets stand for equivalent positions of atoms as defined in Table III-1.

TABLE III-4

The nature of thermal ellipsoid of some compounds with thortveitite structure

β-$Cu_2P_2O_7$

	RMS (Å)	Direction cosine		
Cu	0.179	-0.9	-0.0	0.69
	0.081	-0.0	1.0	0.000
	0.064	-.43	0.0	-0.72
P	0.096	0.0	1.0	0.0
	0.094	1.0	0.0	-.40
	0.079	-.08	0.0	0.92
01	0.346	0.0	1.0	0.0
	0.172	-0.14	0.0	-.89
	0.074	0.99	-0.0	-.45
02	0.097	-.85	-0.0	0.77
	0.093	-0.0	1.0	0.0
	0.079	-.5241	0.0	-.64
03	.182	1.0	-.03	-.42
	.152	.09	.66	.66

non positive definite

$Cd_2V_2O_7$

Cd	0.103	0.65	-0.0	-.88
	0.096	0.76	0.0	0.46
	0.094	0.0	1.0	0.0

(continued next page)

TABLE III-4 (continued)

	RMS (Å)	Direction cosine		
V	0.089	-0.0	-1.0	0.0
	0.087	0.981	-0.0	-.16
	0.066	-.06	-0.0	0.98
01	.273	0.41	0.0	.793
	.168	0.0	1.0	0.0
	non positive definite			
02	.149	.67	-0.0	-.87
	.116	0.0	1.0	-0.0
	.019	-.738	-0.0	-.49
03	.168	.75	.23	.43
	.105	.63	-.49	-.72
	.065	-.17	-.83	.54

BIBLIOGRAPHY

Au, P.K.L. and Calvo, C., Can. J. of Chem., Vol. 45, 2297 (1967).

Baur, W.H., Trans. of the Amer. Cryst. Assoc., Vol. 6, 129-155 (1970).

Brown, I. D. and Calvo, C., J. of Solid State Chem., 1, 173-79 (1970).

Busing, W.R. and Levy, H.A., Acta Cryst. 17, 142 (1964).

Calvo, C.,Leung, J.S. and Datars, W.R., J. Chem. Phys. 46, 797-803 (1967).

Calvo, C., Private Communication (1967).

Calvo, C.,Can. J. Chem. 1139-45, Vol. 43 (1965a).

Calvo, C., Can. J. Chem., 1147-53, Vol. 43 (1965b).

Calvo, C. and Neelkantan, K., Can. J. of Chem., 48, No. 6, 890 (1970).

Chambers, J. G., Datars, W.R. and Calvo, C., J. Chem. Phys. 41, 806 (1964).

Cruickshank, D.W.J., J. Chem. Soc. 5486 (1961).

Cruickshank, D.W.J., Lynton, H. and Barclay, G.A., Acta Cryst. 15, 491 (1962).

Cruickshank, D.W.J., Pilling, D.E., Bujosa, A., Lovell, F.M. and Truter, M.R., "Computing Methods and the Phase Problem in X-ray Crystal Analysis", Pergamon Press, London (1961).

Datars, W.R. and Calvo, C., J. of Chem. Phys., 47, 3224 (1967).

Ebba Dorm and Bengt-Olav Marinder, Acta Chemica Scandinavica 21, 590-91 (1967).

Gopal, R. and Calvo, C., Private Communication (1970).

Hamilton, W. C., Acta Cryst. 18, 502 (1965).

Kawahara, A., Bull. Soc. fr. Min. Crist. 90, 279 (1967).

Krishnamachari, N. and Calvo, C., Private Communication (1970).

Lazarev, A.N., Izv. Akad. Nauk, S.S.S.R. Otd. Khim. Nauk, 1314 (1962).

Lukaszewicz, K., Bull. De L'Academie Folonaoise Des Sciences Vol. XIV, No. 10 (1966).

Lukaszewicz, K. and Smajkiewicz, R. Roczniki Chemii 35, 741 (1961).

Pietraszko, A. and Lukaszewicz, K., Bull. De L'Academie Polonaise Des Sciences Vol. XVI, No. 4 (1968).

Robertson, B.E. and Calvo, C., Can. J. of Chem., 46, 605 (1968).

Robertson, B. E., Ph.D. Thesis, McMaster University (1967).

Robertson, B.E. and Calvo, C., Acta Cryst. 22, 665 (1967).

Stager, C.V. and Atkinson, R.J., Canadian J. of Physics, 47, 1557 (1969).

Woolfson, M.M., An introduction to X-ray crystallography, Cambridge University Press (1970).

Wyckoff, R.W.G., "Crystal Structures" Volume 3, Wiley (Interscience) New York, 1960.

Zachariasen, W.H., Z. Kristallogr., 73, 1 (1930).